Article Type: Original Article

Assembly, trafficking and function of α1β2γ2 $GABA_A$ receptors are regulated by N-terminal regions, in a subunit-specific manner

Lik-Wei Wong[1,2], Han-Shen Tae[1] and Brett A. Cromer[1¶]

[1]Health Innovation Research Institute, School of Medical Sciences, RMIT University, Melbourne VIC

[2]Department of Pharmacology and Therapeutics, University of Melbourne, Melbourne VIC

[¶] To whom correspondence should be addressed:

Brett A. Cromer, Health Innovation Research Institute, School of Medical Sciences, RMIT University, Bundoora VIC 3082, email: brett.cromer@rmit.edu.au

Abbreviations: GABA, γ-amino butyric acid; pLGIC, pentameric ligand-gated ion channel; $GABA_AR$, type A GABA-activated pLGIC; $GABA_CR$, type C GABA-activated pLGIC; GlyR, glycine receptor pLGIC; nAChR, nicotinic acetylcholine receptor pLGIC; $5HT_3R$, serotonin receptors pLGIC; GluCl, glutamate-gated chloride channel; AChBP, acetylcholine-binding protein; ELIC, pLGIC from *Erwinia chrysanthemi;* GLIC, pLGIC from *Gloebacter violaceus*; ECD, extracellular domain; TM trans-membrane region; CDP, chlordiazepoxide; ΔEx, deletion from the N-terminus to the end of the predicted N-terminal extension; ΔExαH, deletion from the N-terminus to just before dileucine motif in putative α-helix; ΔExαH+3, deletion from the N-terminus to the end of the putative α-helix (removing dileucine motif)

Abstract

$GABA_A$ receptors are pentameric ligand-gated ion channels (pLGIC) that mediate inhibitory fast synaptic transmission in the central nervous system. Consistent with recent pLGIC structures, sequence analysis predicts an α-helix near the N-terminus of each $GABA_A$ receptor subunit. Preceding each α-helix are 8-36 additional residues, which we term the N-terminal extension. In homomeric $GABA_C$ receptors and nicotinic acetylcholine receptors (nAChR), the N-terminal α-helix is functionally essential. Here we determined the role of the N-terminal extension and putative α-helix in heteromeric α1β2γ2 $GABA_A$ receptors. This role

This article has been accepted for publication and undergone full peer review but has not been through the copyediting, typesetting, pagination and proofreading process which may lead to differences between this version and the Version of Record. Please cite this article as an 'Accepted Article', doi: 10.1111/jnc.13175

was most prominent in the α1 subunit, with deletion of the N-terminal extension or further deletion of the putative α-helix both dramatically reduced the number of functional receptors at the cell surface. Conversely, deletion of the β2 or γ2 N-terminal extension had little effect on the number of functional cell-surface receptors. Additional deletion of the putative α-helix in the β2 or γ2 subunits did, however, decrease both functional cell surface receptors and incorporation of the γ2 subunit into mature receptors. In the β2 subunit only, α-helix deletions affected GABA sensitivity and desensitization. Our findings demonstrate that N-terminal extensions and α-helices make key subunit-specific contributions to assembly, consistent with both regions being involved in inter-subunit interactions.

Introduction

$GABA_A$ receptors ($GABA_ARs$) are anion-selective members of the pentameric ligand-gated ion channel (pLGIC) superfamily. They are the primary mediators of fast inhibitory synaptic transmission in the human central nervous system. The pLGIC superfamily also includes anion-selective $GABA_CR$ and glycine receptors (GlyR) and cation-selective nicotinic acetylcholine receptors (nAChR) and serotonin receptors ($5HT_3R$) (Barnard et al., 1998; Macdonald and Olsen, 1994; Thompson et al., 2010). $GABA_ARs$ are allosterically modulated by a range of pharmacologically and clinically important drugs, such as benzodiazepines, barbiturates, neurosteroids, anaesthetics and convulsants (Korpi et al., 2002; Reynolds et al., 2003; Sieghart, 1995). Functional $GABA_ARs$ are thought to be heteropentamers assembled from at least 16 subunit isoforms identified thus far, including α(1-6), β(1-3), γ(1-3), δ, ε, π and θ (Barnard et al., 1998; Macdonald and Olsen, 1994). This gives rise to a great variety of $GABA_AR$ subtypes with different subunit composition, cellular distribution and pharmacology properties. The majority of native receptors are, however, composed of two α, two β and one γ subunit with the α1β2γ2 subunit combination being the most prevalent $GABA_ARs$ in the human brain (Ernst et al., 2005; Olsen and Sieghart, 2009; Sieghart, 1995).

Homopentameric ion channels can be formed from β1 or β3 subunits alone but they are not GABA-activated (Krishek et al., 1996; Wooltorton et al., 1997b). Unlike αγ or βγ, an αβ subunit composition can form functional GABA-activated $GABA_ARs$ *in vitro.* When the γ2 subunit is present, however, αβγ $GABA_ARs$ are produced preferentially over αβ $GABA_ARs$

(Angelotti et al., 1993; Verdoorn et al., 1990). This preference for αβγ $GABA_A$Rs can be further biased by transfecting with larger amounts of γ2 relative to α and β subunit cDNAs (Boileau et al., 2002). As benzodiazepines bind at the interface between the α and γ2 subunits, the presence of the γ2 subunit, together with α and β subunits, is essential for benzodiazepine sensitivity (Cromer et al., 2002; Pritchett et al., 1989; Sigel et al., 1990; Sigel and Buhr, 1997). This has also been confirmed *in vivo* with γ2 subunit knockout mice (Gunther et al., 1995). A markedly lower sensitivity to inhibition by Zn^{2+} is another hallmark of α1β2γ2 $GABA_A$Rs compared to α1β2 $GABA_A$Rs that lack a γ subunit (Draguhn et al., 1990; Saxena and Macdonald, 1994). Two Zn^{2+} binding sites have been identified at the interface between the α1 and β subunits in the extracellular domain and a third, which has the highest affinity for Zn^{2+}, within the channel lumen (Horenstein and Akabas, 1998; Hosie et al., 2003; Wooltorton et al., 1997a). Incorporation of the γ2 subunit into $GABA_A$Rs disrupts one of two Zn^{2+} binding sites in the extracellular domain and the high-affinity Zn^{2+}-binding site in the channel lumen, thus decreasing Zn^{2+} sensitivity (Hosie et al., 2003).

The first high resolution structure relevant to pLGICs was of a molluscan acetylcholine-binding protein (AChBP) with homology to the extracellular domain of nAChR (Brejc et al., 2001). Since then, our understanding of pLGIC structure at atomic resolution has advanced dramatically. The first structure of a full length pLGIC at a resolution sufficient to build an atomic model was resolved from the cryo-electron microscopy of *Torpedo* nAChR at 4 Å resolution (Miyazawa et al., 2003; Unwin, 2005). The identification of prokaryotic pLGICs (Tasneem et al., 2005) led to structures, at high resolution, of pLGICs from *Erwinia chrysanthemi* (ELIC) (Hilf and Dutzler, 2008) and *Gloebacter violaceus* (GLIC) (Bocquet et al., 2009; Hilf and Dutzler, 2009). The first X-ray structure of an anion-selective pLGIC, an invertebrate glutamate-gated chloride channel (GluCl), was resolved in 2011 in an apparently open state (Hibbs and Gouaux, 2011). Recently a GluCl closed state structure was resolved (Althoff et al., 2014) and the first structures of mammalian pLGICS were determined; a homomeric β3 $GABA_A$R (Miller and Aricescu, 2014) and a homomeric $5HT3_A$R (Hassaine et al., 2014). These structures provide a remarkably consistent picture of pLGIC structure.

Each pLGIC subunit comprises a large N-terminal extracellular domain (ECD), followed by four transmembrane α-helices (TM1-4) that form the channel domain and a variable intracellular domain between TM3 and TM4. The intracellular domain is basically absent in prokaryotic pLGICs, with a short loop linking TM3 and TM4. All available structural information shows the core of the ECD is a β-sandwich of ten β-strands. The agonist-binding site is formed near the mid-point of the ECD at the interface between two subunits, involving the principal or (+) face of one subunit and the complimentary or (-) face of the other (Figure 1A). The so-called "loop C", between β strands 9 and 10 of the (+) side subunit, forms a lid over the agonist-binding site. An N-terminal α-helix precedes the β-sandwich in all eukaryotic structures but is absent in prokaryotic structures, raising the question of whether this helix is essential in eukaryotic pLGICs.

In addressing this question, the N-terminal α-helix has been shown to be essential in homomeric α7 nAChRs (Bar-Lev et al., 2011; Castillo et al., 2009), largely due to an important role in receptor assembly and trafficking to the cell surface. We have recently reported similar findings for the putative N-terminal α-helix in ρ1 $GABA_CR$ (Wong et al., 2014). We also found that 46 residues (we term the "N-terminal extension") preceding this putative α-helix were not functionally essential but contributed to the efficiency of receptor assembly and trafficking and to agonist cooperativity (Wong et al., 2014). Here we investigate the role of the N-terminal extension and putative N-terminal α-helix in heteromeric $GABA_AR$ and whether this role is subunit dependent. We used the natively common α1β2γ2 $GABA_AR$ as a model. In each subunit, deletions of the N-terminal extension and the N-terminal α-helix were created. Additional variants included or removed a conserved di-leucine motif that is important in nAChR assembly (Castillo et al., 2009). We demonstrate that the role of these segments is strongly subunit specific. The α1 N-terminal extension is a key determinant of receptor assembly. Conversely, the β2 and γ2 α-helices are important for incorporation of the γ2 subunit.

Materials and methods

Construction of α1β2γ2 GABAAR Mutants

The cDNAs encoding human α1, β2 and γ2 $GABA_AR$ subunit subtypes were individually subcloned into the pCDNA3.1 expression vector. Mutations of $GABA_AR$ subunits were incorporated using the QuickChange® site-directed mutagenesis kit (Stratagene, La Jolla, CA), according to manufacturers instructions. All constructs were verified by sequencing (Australian Genome Research Facility Ltd).

Cell Culture and Transfection

Human embryonic kidney (HEK-293T, from ATCC CRL-3216) cells were incubated at 37 ˚C in a humidified 5% CO_2 incubator and grown in Dulbecco's Modified Eagle Medium (Invitrogen, Life Technologies), supplemented with 10% fetal bovine serum (SAFC Biosciences) and penicillin/streptomycin (100 IU/ml). For expression of wild-type (WT) or mutant α1β2γ2 $GABA_ARs$, HEK-293T, cells in 6-well tissue culture-treated plates (Corning, NY) were transfected with 4 μg of subunit cDNAs at a ratio of 1:1:3 (α1:β2:γ2), using a modified calcium phosphate transfection method (Jordan and Wurm, 2004). Medium was removed and replaced with fresh growth medium 4 h after transfection. The cells were then incubated at 37 ˚C for 36-48 h prior to experiments.

Flow Cytometry Analysis

Flow cytometry was performed to examine the surface and total expression of $GABA_AR$ subunits. Transiently transfected cells were collected in phosphate-buffered saline (PBS) and washed twice with PBS on ice. Cells were kept on ice for all subsequent steps. For detection of total α1β2γ2 expression, cells were fixed with 4% paraformaldehyde for 20 min, then permeabilised with 0.2% Triton X-100 (Sigma-Aldrich, USA) for 15 min and washed again with PBS. For detection of cell-surface α1β2γ2 receptors, cells were not fixed or permeabilised prior to antibody staining. All cells were blocked with 10% horse serum (Gibco, Life Technologies) in PBS for 1 h, then incubated with a 1/200 dilution of mouse monoclonal anti-$GABA_AR$ α chain, MAB339 (Millipore) or rabbit polyclonal anti-$GABA_AR$ γ2, ab82970 (Abcam) for 1 h, followed by two 15 min washes in PBS. Cells were then

incubated in a 1/200 dilution of secondary goat anti-mouse antibody Alexafluor® 633 (Invitrogen, Life Technologies) or goat anti-rabbit antibody Alexafluor® 488 (Invitrogen, Life Technologies) in the dark for 1 h, followed by two 15 min washes in PBS. Cell-surface stained cells were then fixed with 4% paraformaldehyde for 20 min and washed with PBS for 15 min. The fluorescence intensity (FI) of 10,000 cells from each sample was measured using a BD FACS Canto II (BD Biosciences) flow cytometer. Each experiment included negative control untransfected cells and positive control α1β2γ2 WT transfected cells stained in the same manner as mutant samples. The FI of untransfected cells was substracted from the mean FI of all other samples and the resulting mean fluorescence of each mutant expressed as a percentage of α1β2γ2 WT within each experiment. These percentages were averaged across multiple experiments.

Electrophysiology

Electrophysiological recordings were performed on transiently-transfected HEK-293T cells expressing α1β2γ2 $GABA_A$Rs, using ensemble microfluidic plates in a 96-well plate automated electrophysiology platform (IonFlux-16^{TM} System) developed by Fluxion Biosciences, USA (Chen et al., 2012; Golden et al., 2011; Spencer et al., 2012). Cells were washed with PBS and then incubated with TrypLE (Invitrogen, Life Technologies) for 2-5 min, resuspended in serum free media (Invitrogen, Life Technologies), harvested by centrifugation at 1000 rpm for 2 min and washed three times with extracellular solution (in mM: 138 NaCl, 4 KCl, 1 MgCl2, 1.8 CaCl2, 10 HEPES, 5.6 glucose, pH 7.45 with NaOH). Finally, cells were resuspended in extracellular solution at a concentration of 2–5 million cells/ml for electrophysiology. The intracellular solution was (in mM): 15 NaCl, 60 KCl, 70 KF, 5 EGTA, 5 HEPES, pH 7.25 with KOH. GABA dilutions in extracellular solution were prepared on the day of experiment from a frozen 1M stock solution. Whole-cell currents were recorded from populations of up to 20 cells voltage-clamped at -80 mV. Each GABA application lasted for 3 s, with a 2 min wash between applications to allow the receptors to recover from desensitization. Recordings were performed at room temperature (22-25°C).

The kinetics of macroscopic desensitization were determined by applying a saturating GABA concentration (1 mM) for 10 s to HEK-293T cells expressing WT or mutant α1β2γ2 $GABA_A$Rs. For analysis of desensitization, the time of onset of desensitization was set to zero and the time course of desensitization was fitted by exponential components with a simplex algorithm (Axograph Software).

To determine γ2 subunit incorporation into α1β2γ2 $GABA_A$Rs, we tested the inhibitory effect of 30 μM $ZnCl_2$ on saturating 1mM GABA-elicited currents in HEK-293T cells expressing WT or mutant $GABA_A$R. Cells were exposed twice to 1 mM GABA then pre-incubated with extracellular solution containing Zn^{2+} for 2 min, before being exposed to 30 μM Zn^{2+} together with 1 mM GABA for 3 s. Cells were then washed back into extracellular solution to recover from Zn^{2+} inhibition and retested. Percentage inhibition by Zn^{2+} was calculated from peak currents in the presence ($I_{GABA+ZINC}$) and absence (I_{GABA}) of Zn^{2+}, using the equation (I_{GABA} - $I_{GABA+ZINC}$) / I_{GABA} x 100%. We also determined benzodiazepine sensitivity by measuring potentiation by chlordiazepoxide (CDP) of 6 μM GABA-elicited currents in HEK-293T cells expressing WT or mutant $GABA_A$Rs. Cells were exposed three times to 6 μM GABA for 3 s with a 2 min wash between each application to ensure a stable response. Cells were then exposed to 1 μM CDP together with 6 μM GABA for 3 s. Percentage of CDP potentiation (CDP potentiation %) was calculated from peak currents in the presence ($I_{GABA+CDP}$) or absence (I_{GABA}) of CDP, using the equation ($I_{GABA+CDP}$ - I_{GABA}) / I_{GABA} x 100%.

Data analysis and statistics

Secondary structure predictions were carried out with Jpred3 (Cole et al., 2008) (http://www.compbio.dundee.ac.uk/www-jpred/). Electrophysiology data were analysed with integrated Fluxion software and Axograph X (http://www.axograph.com/). For each experiment, complete GABA dose response data were recorded and peak currents fitted to the Hill equation. EC_{50} and Hill coefficients from these fits were averaged from several experiments. Prism 6 (GraphPad Software Inc. La Jolla, CA) was used for curve fitting to data and statistical analysis. Numerical data are presented as means ± SEM. Statistical differences to WT α1β2γ2 $GABA_A$Rs were estimated using one-way ANOVA and Dunnett's

post-hoc multiple comparisons test, with $p<0.05$ considered indicative of a significant difference (GraphPad Prism Software).

Results

Secondary structure predictions, using Jpred3 (Cole et al., 2008), consistently predict an N-terminal α-helix (highlighted in yellow, Figure 1B) in each subunit of the α1β2γ2 $GABA_AR$. These predictions aligned closely with each other and with α-helices in resolved structures (highlighted in cyan, Figure 1B), including the recent structure of a homomeric β3 $GABA_AR$ (Miller and Aricescu, 2014). Unlike nAChRs, mature subunits of $GABA_ARs$ (and GluCl) have a substantial "N-terminal extension" prior to the putative N-terminal α-helix. To determine the functional role of these N-terminal regions, we created a series of deletion mutants of α1, β2 and γ2 $GABA_AR$ subunits, using a definition of the putative N-terminal α-helix that is consistent across all subunits (highlighted in yellow, Figure 1C). Firstly, we created deletions of each subunit, defined as ΔEx, that lack residues corresponding to the predicted extension. We created two further deletions that extend into the N-terminal α-helix. The first construct, defined as ΔExαH, lacks residues from the N-terminus to the amino acid prior to a relatively conserved di-leucine motif at the C-terminal end of the putative α-helix. The second construct, defined as ΔExαH+3, completely removes the predicted N-terminal extension and α-helix, including the di-leucine motif. To ensure fidelity of signal peptide cleavage, the first mature residue (Q1) was retained in all deletion constructs.

Deletions to the N-terminal extension do not affect functional properties of $GABA_ARs$

GABA-activated channel function of WT and mutant $GABA_ARs$ was measured electrophysiologically using an automated microfluidic system (IonFlux-16) that records total whole-cell current from a population of up to 20 cells. Typical current recordings are shown in Figure 2A and normalised average GABA dose-response curves in Figure 2B. The GABA concentration required to elicit half-maximum response (GABA EC_{50}) for α1β2γ2 $GABA_AR$ was 11.0 ± 1.2 with a Hill coefficient of 1.1 ± 0.1 (Table 1). The GABA EC_{50} (0.5 ± 0.2 μM) for α1β2 $GABA_AR$ was significantly smaller ($p<0.0001$) compared to α1β2γ2 $GABA_AR$. Consistent with previous studies for α1β2 $GABA_ARs$ (Angelotti et al., 1993; Boileau et al., 2003), the Hill coefficient for α1β2 (0.9 ± 0.2) was similar to that of α1β2γ2 $GABA_AR$ (Table

1). Mutant α1β2γ2 $GABA_A$Rs with deletions of the N-terminal extension in each single subunit were functional and showed dose-dependent GABA-gated currents (Figure 2A). The GABA EC_{50} (μM) for α1(ΔEx)β2γ2, α1β2(ΔEx)γ2 and α1β2γ2(ΔEx) was 11.1 ± 0.5, 8.0 ± 0.5 and 8.0 ± 1.0 respectively with Hill coefficients ranging from 1.2 to 1.3 (Figure 2B and Table 1). Neither the GABA EC_{50} nor the Hill coefficients of any of the N-terminal extension deletion mutants were significantly different to that of α1β2γ2 WT (Table 1).

Most $GABA_A$Rs show substantial desensitization in the continued presence of agonist. The rate of desensitization reflects the relative stability and kinetics of conformational changes between different channel states. To examine whether deletion of the N-terminal extension affected desensitization, 1mM GABA was applied for 10 s and the desensitization phase was well fitted with a single exponential decay. Using the 20-cell IonFlux-16 plate format, the time for 10-90% solution exchange is approximately 50 ms (data not shown), a rate of GABA application that may obscure faster components of desensitization. With this constraint in mind, the desensitization rates for α1β2(ΔEx)γ2 (1.5 ± 0.1 s) and α1β2γ2(ΔEx) (1.2 ± 0.1 s) were not found to be significantly different to α1β2γ2 WT (1.5 ± 0.1 s) (Supplementary Figure 1). As the current amplitudes were relatively small for the extension deletion of the α1 subunit in α1(ΔEx)β2γ2, it was difficult to reliably measure the rate of desensitization for this mutant.

As small whole-cell currents may indicate a deficit in $GABA_A$R function, subunit folding, assembly or trafficking, we next quantified the effect of each deletion on peak whole-cell currents. Although there may be large variability in the magnitude of whole-cell currents from transfected cells, this can be greatly reduced by measurement from a cell population, such as up to twenty cells in the current study. The population whole-cell peak current (I_{MAX}) for α1(ΔEx)β2γ2 was significantly reduced ($p<0.0001$) to 16 ± 5% of α1β2γ2 WT (Table 1). There was, however, no significant difference in peak current for α1β2(ΔEx)γ2 (81 ± 8% of α1β2γ2 WT) or α1β2γ2(ΔEx) (89 ± 14% of α1β2γ2 WT) relative to α1β2γ2 WT (Table 1). Taken together, these data indicate that the N-terminal extension is not important for GABA-activation of ion channel function but is important, specifically in the α subunit, for achieving the maximum level of functional $GABA_A$Rs.

Deletion of the α subunit N-terminal extension decreases cell surface α1β2γ2 $GABA_A$Rs

To determine whether the reduced whole-cell peak current of the α1(ΔEx)β2γ2 mutant was due to a functional defect, decreased total subunit expression or decreased receptor trafficking to the plasma membrane, we measured cell surface and total expression of WT and N-terminal extension deletions of α1β2γ2 $GABA_A$Rs by indirect immunofluorescent labelling of intact and permeabilised cells, respectively. Two anti-$GABA_A$R subunit primary antibodies were used, anti-α chain (MAB339) and anti-γ2 (ab82970) that bind with high affinity to the extracellular domain of α1 and γ2 $GABA_A$R subunits, respectively (Figure 3). These antibodies recognize epitopes in the N-terminal segments that are deleted in our ΔEx constructs, so cannot be used to detect these subunits directly. Consequently, we detected α1(ΔEx)β2γ2 $GABA_A$Rs with the anti-γ2 antibody and α1β2γ2(ΔEx) with the anti-α chain antibody. The α1β2(ΔEx)γ2 $GABA_A$R was detected with both antibodies.

The degree of immunofluorescent labelling of each cell in a transfected population was measured using flow cytometry. Histograms of cell surface (intact cells) and total (permeabilised cells) anti-α subunit immunofluorescence labelling (Figure 3A) for cells expressing α1β2(ΔEx)γ2 and α1β2γ2(ΔEx) and α1β2γ2 WT were all markedly shifted to the right relative to untransfected cells. The shift appeared less for the permeabilised cells than intact cells, largely due to higher non-specific staining of untransfected cells when permeabilised. There was no clear distinction between untransfected and transfected populations of cells, indicating the rate of transfection was high but with a large variation in receptor expression. Consequently, the mean fluorescence of the whole population of cells was used to compare levels of deletion mutants to that of WT $GABA_A$Rs. The amount of α1 subunit detected at the cell surface relative to α1β2γ2 WT was 80 ± 6% for α1β2(ΔEx)γ2 and 113 ± 13% for α1β2γ2(ΔEx). Neither was significantly different to α1β2γ2 WT (Figure 3A). There was also no significant difference in total receptor expression relative to α1β2γ2 WT, for either α1β2(ΔEx)γ2 or α1β2γ2(ΔEx), being 91 ± 4% and 129 ± 2% of α1β2γ2 WT respectively (Figure 3A). These results are consistent with a lack of effect of either of these two deletions on the magnitude of whole-cell currents.

In agreement with the anti-α chain antibody results, detection of α1β2(ΔEx)γ2 with the anti-γ2 antibody showed no significant difference to α1β2γ2 WT at either the cell surface (91 ± 11%) or total receptor expression (92 ± 9%) (Figure 3B). However, deletion of the N-terminal extension in the α1 subunit (α1(ΔEx)β2γ2) markedly and significantly ($p<0.0001$) reduced the amount of γ2 subunit detected at the cell surface to 19 ± 4% of α1β2γ2 WT. This finding is consistent with the reduced whole-cell currents reported above. The total expression of the γ2 subunit for α1(ΔEx)β2γ2 (90 ± 10% of α1β2γ2 WT) was similar to α1β2γ2 WT (Figure 3B). These data may be explained by an effect of α1 subunit N-terminal extension deletion on the efficiency of receptor assembly and trafficking to the cell surface. Alternatively, as,cell-surface receptors for this mutant were only detected with the anti-γ2 antibody the incorporation of the γ2 subunit into cell surface receptors may be reduced. Indeed, α1β2 $GABA_A$Rs that lack the γ2 subunit are fully functional GABA-activated channels but have altered pharmacology relative to α1β2γ2 $GABA_A$Rs (Draguhn et al., 1990; Pritchett et al., 1989).

Deletions of the N-terminal extension do not affect γ2 subunit incorporation into $GABA_A$Rs

To examine whether deletions of the N-terminal extension alter γ2 subunit incorporation into $GABA_A$Rs, we tested their effect on sensitivity to Zn^{2+} inhibition and benzodiazepine potentiation (Figure 4). We recapitulated here that presence of the γ2 subunit in $GABA_A$Rs confers sensitivity to benzodiazepine potentiation and reduced sensitivity to inhibition by Zn^{2+} (Draguhn et al., 1990; Pritchett et al., 1989). Addition of 30 μM Zn^{2+} inhibited peak whole cell currents in response to 1 mM GABA by 18 ± 0 2% in HEK-293T cells expressing α1β2γ2 $GABA_A$Rs, significantly less ($p<0.0001$) than the 79 ± 0 2% inhibition observed in cells expressing α1β2 $GABA_A$Rs (Figure 4, Table 1). Correspondingly, the benzodiazepine chlordiazepoxide (CDP), at 1 μM, potentiated peak whole-cell currents in response to 6 μM GABA by 54 ± 5% in cells expressing α1β2γ2 $GABA_A$Rs, significantly greater ($p<0.0001$) than the absence of potentiation (1 ± 1%) in cells expressing α1β2 $GABA_A$Rs (Figure 4, Table 1).

We next tested the effect of each of the three N-terminal extension deletions on Zn^{2+} inhibition and CDP potentiation under the conditions described above. Each of the deletion mutants showed similar sensitivity to both Zn^{2+} inhibition and CDP potentiation as α1β2γ2 WT $GABA_A$Rs. 30 μM Zn^{2+} inhibited peak whole-cell currents activated by 1mM GABA by 15 ± 4%, 13 ± 4% and 19 ± 4% for α1(ΔEx)β2γ2, α1β2(ΔEx)γ2 and α1β2γ2(ΔEx), respectively (Figure 4A). None were significantly different to Zn^{2+} inhibition of α1β2γ2 WT (Table 1). Furthermore, 1 μM CDP potentiated 6 μM GABA-activated currents by 46 ± 10%, 39 ± 7% and 45 ± 7% for α1(ΔEx)β2γ2, α1β2(ΔEx)γ2 and α1β2γ2(ΔEx), respectively (Table 1). Again none were significantly different to CDP potentiation of α1β2γ2 WT. Taken together, these results are clear evidence that incorporation of the γ2 subunit into cell surface $GABA_A$Rs was not compromised by the absence of the N-terminal extension in any of the three subunits. In particular, the reduced level of the γ2 subunit detected at the cell surface due to the α1(ΔEx) deletion was not due to a decreased incorporation of the γ2 subunit. Rather, it must reflect a reduced number of $GABA_A$Rs at the cell surface, consistent with the reduced whole-cell peak current in cells expressing α1(ΔEx)β2γ2 $GABA_A$Rs.

N-terminal α-helix deletions, only in the β subunit, affect GABA-activated channel function

We next turned our attention to the role of the putative N-terminal α-helix. Larger deletions from the N-terminus of each subunit to a relatively conserved dileucine motif at the C-terminal end of the putative α-helix, termed ΔExαH, (Figure 1C), removed most of the helix as well as the N-terminal extension. We chose to retain the dileucine motif based on evidence of it having a key role in nAChRs assembly (Castillo et al., 2009). Each ΔExαH deletion was co-transfected with full-length constructs of the other two subunits into HEK-293T cells.

Each of the three ΔExαH mutant subunits produced receptors that showed dose-dependent GABA-gated currents (Figure 5A). The GABA EC_{50} was slightly but significantly reduced ($p<0.05$) to 5.1 ± 2.3 μM for α1(ΔExαH)β2γ2, whilst the EC_{50} of 7.2 ± 1.8 μM for α1β2γ2(ΔExαH) was not significantly different to that for WT (Figure 5A and Table 1). Conversely, for α1β2(ΔExαH)γ2, the GABA EC_{50} (28.1 ± 4.3 μM) showed a significant 2.5 fold increase ($p<0.05$) relative to α1β2γ2 WT. None of the Hill coefficients, 1.0 ± 0.3 for

α1(ΔExαH)β2γ2, 1.0 ± 0.1 for α1β2(ΔExαH)γ2 and 1.0 ± 0.2 for α1β2γ2(ΔExαH), were significantly different to that of α1β2γ2 WT (1.1 ± 0.1) (Figure 5A and Table 1).

Kinetic analysis of current desensitization during exposure to 1 mM GABA for 10 s (Supplementary Figure 1) revealed that $GABA_A$Rs with a ΔExαH deletion in the β2 subunit exhibited a desensitization rate of 2.5 ± 0.1 s that was significantly slower ($p<0.001$) than that of α1β2γ2 WT (1.5 ± 0.1 s). The plateau of desensitized current for the β2 deletion was also significantly increased to more than double that of WT (Supplementary Figure 1). Both kinetic changes suggest a stabilisation of the open state relative to the desensitized state. The desensitization rate (1.6 ± 0.1 s) for α1β2γ2(ΔExαH) was, however, similar to α1β2γ2 WT (Supplementary Figure 1). As mention above, any changes in faster components of desensitization may be hidden by the rate of GABA application. Again, currents for α1(ΔExαH)β2γ2 were too small to provide reliable measures of desensitization. These results indicate that only in the β subunit does the ΔExαH deletion significantly affect GABA-activation of ion channel function.

Deletions to the N-terminal α-helix in any subunit decrease $GABA_A$Rs at the cell surface

Similar to deletion of the N-terminal extension, the ΔExαH deletion in the α subunit significantly reduced ($p<0.0001$), the population whole-cell peak current (I_{MAX}) of α1(ΔExαH)β2γ2 to 10 ± 3% of α1β2γ2 WT (Table 1). The larger ΔExαH deletion in either the β or γ subunits also significantly reduced peak currents to 40 ± 3% and 70 ± 6% of α1β2γ2 WT for α1β2(ΔExαH)γ2 and α1β2γ2(ΔExαH), respectively (Table 1).

As above, to investigate the cause of reduced whole-cell currents in deletion mutants we measured cell surface and total subunit expression by flow cytometry using anti-α or anti-γ2 antibodies (Supplementary Figure 2). Detection with the anti-α antibody (Figure 6A) showed the level of the α subunit at the cell surface to be significantly decreased to 10 ± 3% of α1β2γ2 WT for α1β2(ΔExαH)γ2 ($p<0.0001$) and 54 ± 5% of α1β2γ2 WT for α1β2γ2(ΔExαH) ($p<0.01$). Detection of the γ subunit at the cell surface for α1β2(ΔExαH)γ2 was also significantly reduced to 16 ± 6 % of α1β2γ2 WT, consistent with the decreased detection of

the α subunit. Together, the lower cell surface detection of α and γ subunits provide clear evidence that lower levels of cell surface receptors is the reason for reduced whole-cell currents in α1β2(ΔExαH)γ2 receptors. Indeed, the fractional decrease in subunits detected at the cell surface was more than the decrease in peak currents. Detection of the γ subunit at the cell surface for α1(ΔEx)αHβ2γ2 was also significantly reduced ($p<0.0001$) to 11 ± 2% of α1β2γ2 WT (Figure 6B), correlating closely with the reduction in whole-cell currents for this mutant receptor. Decreased detection of surface γ subunits due to the α1(ΔEx)αH deletion is similar to that caused by the smaller α1(ΔEx) deletion.

For all ΔExαH deletions the total subunits detected from permeabilised cells were similar to α1β2γ2 WT, for both the α subunit (110 ± 13% and 105 ± 7% of α1β2γ2 WT for α1β2(ΔExαH)γ2 and α1β2γ2(ΔExαH), respectively (Figure 6A)) and the γ subunit (107 ± 16% and 102 ± 17% of α1β2γ2 WT for α1(ΔExαH)β2γ2 and α1β2(ΔExαH)γ2, respectively (Figure 6B)). Thus a deficiency in trafficking and/or assembly does not appear to result in subunit degradation.

Deletions to the N-terminal α-helix in β or γ subunits decrease γ2 incorporation into functional $GABA_A$Rs

We again used inhibition by 30 μM Zn^{2+} and potentiation by 1 μM CDP as measures of γ2 subunit incorporation into functional receptors. Currents for the α1(ΔExαH) deletion were inhibited by Zn^{2+} to 21 ± 5% of control, similar to α1β2γ2 WT (Figure 6C and Table 1). In agreement with the Zn^{2+} inhibition, CDP potentiation (48 ± 6%) for α1(ΔExαH)β2γ2 was not significantly different to α1β2γ2 WT (Figure 6D and Table 1). Thus the α1(ΔExαH) deletion, which had the greatest effect on reducing the number of γ subunits at the cell surface, did not affect incorporation of γ2 subunit into mutant receptors.

Conversely, ΔExαH deletions in the β2 or γ2 subunit showed increased Zn^{2+} inhibition to 43 ± 3% and 61 ± 5% for α1β2(ΔExαH)γ2 and α1β2γ2(ΔExαH), respectively (Figure 6C and Table 1), both significantly greater ($p<0.0001$) than α1β2γ2 WT. Furthermore, ΔExαH deletions in either the β2 or γ2 subunit significantly decreased potentiation by CDP to 15 ±

4% for α1β2(ΔExαH)γ2 ($p<0.001$) and 5 ± 2% for α1β2γ2(ΔExαH) ($p<0.0001$), relative to 54 ± 5% for α1β2γ2 WT (Figure 6D and Table 1). Both the higher Zn^{2+} inhibition and lower benzodiazepine potentiation indicate that functional α1β2(ΔExαH)γ2 and α1β2γ2(ΔExαH) $GABA_A$Rs had incorporated significantly less γ2 subunit. Thus, in both cases, a significant proportion of functional receptors at the cell surface were α1β2 receptors. The effects on both Zn^{2+} inhibition and CDP potentiation were greatest in the γ2(ΔExαH) deletion, indicating that very few functional receptors would actually contain this deleted γ2 subunit.

Complete deletion of the N-terminal helix in α1 or β2 subunits does not abolish function

To test the role of the three remaining, LLX, C-terminal residues of the putative N-terminal α-helix, larger deletions were made, termed ΔExαH+3. These deleted from the N-terminus to the C-terminal end of the putative α-helix, thus removing the di-leucine motif. As the γ2(ΔExαH) deletion greatly reduced γ2 subunit incorporation, we did not make a larger ΔExαH+3 deletion for the γ2 subunit. When coexpressed with the other two WT subunits, a ΔExαH+3 deletion in either the α1 or β2 subunit produced functional $GABA_A$Rs (Table 1). Whole-cell currents from HEK-293T cells expressing α1(ΔExαH+3)β2γ2 were very small, with a significant decrease to 9 ± 1% of α1β2γ2 WT ($p<0.0001$). Although the peak currents were clearly GABA dose-dependent, their small size prevented reliable measurement of a GABA EC_{50} for this mutant receptor. With a similar deletion in the β2 subunit of α1β2(ΔExαH+3)γ2, whole-cell peak currents were also significantly reduced ($p<0.0001$), but only to 40 ± 2% of α1β2γ2 WT (Table 1). The GABA EC_{50} of α1β2(ΔExαH+3)γ2 receptors was 91 ± 19, significantly greater ($p<0.0001$) than that of α1β2γ2 WT. The Hill coefficient (1.0 ± 0.1) was similar to α1β2γ2 WT (Figure 5B and Table 1). Deleting the three extra residues (ΔExαH+3) to completely remove the putative α-helix exacerbates the effects of the slightly small deletions (ΔExαH) in terms of both the α1 subunit effect on smaller peak currents and the β2 subunit effect on reduced sensitivity to GABA. In contrast to previous studies of homomeric pLGICs (Bar-Lev et al., 2011; Castillo et al., 2009; Wong et al., 2014), complete removal of the putative α-helix does not abolish GABA-activated channel function.

$GABA_A$Rs with N-terminal deletions in all subunits retain some function

To compare this study more directly with earlier work on monomeric receptors, we next investigated the effect of N-terminal deletions in all expressed subunits. First, HEK-293T cells were transfected with a ΔEx deletion of α1, β2 and γ2 subunits, denoted as allΔEx $GABA_A$Rs. AllΔEx α1β2γ2 $GABA_A$Rs, without any N-terminal extensions, were functional with a GABA EC_{50} (3.9 ± 1.1 μM), significantly lower ($p<0.01$) than that of α1β2γ2 WT (Figure 5C and Table 1) and a Hill coefficient of 1.1 ± 0.2 that was similar to α1β2γ2 WT. The population whole-cell peak current for this triple deleted allΔEx mutant was significantly reduced ($p<0.0001$) to 12 ± 2% of α1β2γ2 WT (Table 1). The magnitude of this reduction is similar to the deletion of α1ΔEx alone, emphasizing the dominant role of the α1 subunit N-terminal extension.

The larger deletion, denoted allΔExαH, that removed most of the N-terminal α-helix and the N-terminal extension in all subunits of α1β2γ2 $GABA_A$Rs also produced functional receptors (Figure 5C). The allΔExαH GABA EC_{50} was 1.2 ± 0.6 μM, significantly lower ($p<0.05$) than α1β2γ2 WT (Figure 5C and Table 1). Further emphasizing the key role of the α1 subunit N-terminus, similar to the α1(ΔExαH) alone, this triple mutant significantly reduced ($p<0.0001$) population whole-cell peak current to 10 ± 2% of α1β2γ2 WT (Table 1).

Discussion

The α1 N-terminal extension is crucial for receptor assembly and trafficking

We found that deletion of the N-terminal extension in α1 subunit dramatically decreased whole-cell currents to <20% of WT due an equivalent decrease in receptors at the cell surface. Equivalent deletions in either β2 or γ2 subunits had little effect on either the number of receptors at the cell surface or peak GABA-gated whole-cell currents. None of the deletions affected GABA-activated channel function or incorporation of the γ2 subunit into functional $GABA_A$Rs, as measured by benzodiazepine sensitivity and reduced sensitivity to Zn^{2+} inhibition. Simultaneous deletion of the N-terminal extension in all subunits caused a marked reduction in whole-cell currents and cell surface receptors but the reduction was similar to that for the deletion in the α1 subunit alone. Although additional deletions in β2 and γ2 subunits had no additional effect on receptor assembly and trafficking, they did cause

a small decrease in GABA EC_{50}. Taken together, these data show that the N-terminal extension is a major determinant of α1β2γ2 $GABA_AR$ assembly and trafficking, specifically in the α subunit.

The basis for this asymmetry in the importance of the N-terminal extension is not immediately clear but may be rationalised by considering what is known about the process of $GABA_AR$ assembly in the context of $GABA_AR$ structural models. There is clear evidence that the assembly of $GABA_AR$ subunits into mature pentameric receptors is a non-random hierarchical process that predominantly produces receptors with a 2α, 2β, 1γ composition (Angelotti et al., 1993; Bollan et al., 2003; Rabow et al., 1995; Sarto Jackson and Sieghart, 2008; Verdoorn et al., 1990; Wooltorton et al., 1997b). In the context of recent structural information, the predominant arrangement of subunits can be defined as -β+/-α+/-γ+/-β+/-α+/ with the last α+ interfacing with the first -β in a pentameric ring (Figure 1A). Agonist- and benzodiazepine-binding sites are formed at β+/-α and α+/-γ interfaces, respectively, near the middle of the ECD (Cromer et al., 2002). Analysis of assembly intermediates has shown that α, β and γ subunits can all contribute to heterodimers (Klausberger et al., 2001; Tretter et al., 1997), but it has been proposed that assembly may start with a β+/-α hetero-dimer (Sarto Jackson and Sieghart, 2008). Indeed, the ability of agonists or antagonists that bind to the β+/-α interface to act as pharmacological chaperones and increase functional receptors at the cell surface (Eshaq et al., 2010), demonstrates the importance of this interface in a rate-limiting step in receptor assembly. As all eukaryotic pLGIC structures place the N-terminus of the N-terminal α-helix, and hence the N-terminal extension when present, at the (-) face of each subunit, this places the α subunit N-terminal extension close to the β subunit at the same β+/-α interface (Figure 1A). Thus the importance of the α subunit N-terminal extension for receptor assembly and trafficking may be due to an interaction with the β subunit (+) face that enhances β+/-α hetero-dimer formation.

N-terminal α-helices are not functionally essential in heteromeric $GABA_AR$s

In contrast to previous findings for homomeric eukaryotic pLGICs where deletion of the putative N-terminal α-helix abolished functional receptors, we found that some function was retained in heteromeric $GABA_AR$s lacking the putative α-helix in any single subunit or

lacking the bulk of the helix in all subunits. These data indicate that N-terminal α-helices are not essential for subunit folding or receptor function. We did, however, observe reductions in whole-cell currents, cell-surface receptors and γ2 subunit incorporation that further support the contribution of N-terminal α-helices to receptor assembly and trafficking. As all of the α-helix deletions also included deletion of the N-terminal extension, their effects must be compared to the effect of the N-terminal extension alone. Deletion of the α1 subunit from the N-terminus to nearly (ΔExαH) or completely (ΔExαH+3) remove the N-terminal α-helix markedly reduced both cell surface receptors and whole currents. Most of this reduction was due to deletion of the N-terminal extension, with only slight additional decreases due to additional deletions of the N-terminal α-helix. Likewise, the decrease in whole-cell currents due to N-terminal α-helix deletions in all subunits (allΔExαH) was similar to that caused by a similar deletion in the α1 subunit only or indeed by the smaller deletion of just the α1 N-terminal extension. The ΔExαH deletion in all subunits did not abolish function.

In contrast to the α1 subunit, deletion of the N-terminal extension in the β2 subunit had no significant effect on cell surface receptors or whole-cell currents. Further deletions of most (ΔExαH) or all (ΔExαH+3) of the β2 subunit N-terminal α-helix reduced whole-cell currents to 40% of α1β2γ2 WT. Although deletions of the putative α-helix had greater effects on reducing total levels of functional receptors than deletion of just the N-terminal extension, robust whole-cell currents remained, demonstrating that the putative N-terminal α-helices are not essential for functional receptors.

N-terminal α-helices in β2 and γ2 subunits are important for γ2 subunit incorporation

Similar to the β2 subunit, deletion to include most of the N-terminal α-helix in the γ2 subunit (γ2ΔExαH) reduced cell surface receptor levels and whole-cell currents to ≤ 70% of α1β2γ2 WT, whereas deletion of just the N-terminal extension had no significant effect. As functional $GABA_A$Rs can be formed from just α and β subunits (Angelotti et al., 1993; Verdoorn et al., 1990), a key question with any γ2 subunit mutation is whether it affects γ2 incorporation into receptors, producing a mixed population of α1β2 and α1β2γ2 $GABA_A$Rs (Baburin et al., 2008; Baumann et al., 2001; Boileau et al., 2002; Boileau et al., 2003). Indeed, reduced benzodiazepine potentiation and increased Zn^{2+} inhibition, clearly

demonstrated that the γ2(ΔExαH) deletion, removing most of the N-terminal α-helix, markedly reduces γ2 incorporation so that the majority of functional $GABA_A$Rs would be WT α1β2. In this case, the reduced whole-cell current may be partly due to the deleted γ2(ΔExαH) subunit competing unproductively for assembly. The failure of γ2 incorporation due to deletion of most of the γ2 N-terminal α-helix is consistent with assembly and trafficking deficits due to similar deletions in homomeric pLGICs (Wong et al., 2014).

Similar deletion of most of the N-terminal α-helix in the β2 subunit (β2(ΔExαH)) also markedly reduced γ2 incorporation, as demonstrated by decreased benzodiazepine potentiation and increased Zn^{2+} inhibition, but to a lesser extent than the γ2(ΔExαH) deletion. Conversely, the α1(ΔExαH) deletion did not impair γ2 subunit incorporation, despite a dramatic reduction in functional receptors at the cell surface. These differential effects may be explained by noting that structural models place the N-terminus of the putative α-helix at the (-) face of each subunit (Figure 1). Thus, this region in one of the β subunits, but not in the α subunits, could interact with the (+) face of the γ2 subunit and contribute to γ2 incorporation. Likewise, the importance of the γ2 subunit N-terminal α-helix for γ2 incorporation may be explained by a similar interaction with the (-) face of the α subunit.

The di-leucine motif in $GABA_A$Rs does not play a critical role relative to the whole helix

Deletions of the complete N-terminal α-helix (ΔExαH+3), in either α1 or β2 subunits, had no greater effect on peak whole-cell currents than deletions retaining the last three helix residues (ΔExαH), including the di-leucine motif (red in Figure 1B). These data provide no support for a key role for the di-leucine motif above that of the helix as a whole. We designed this comparison based on a previous investigation of α7 nAChRs (Castillo et al., 2009). They found that single mutations within the α-helix, particularly of Leu11 that aligns with the first residue in the di-leucine motif, had similar effects to complete α-helix deletion in abolishing functional cell-surface receptors. In GluCl, this equivalent leucine residue is buried against the top of the β-sandwich (Hibbs and Gouaux, 2011). Interestingly related single mutations also abolished functional cell surface 5HT3Rs but not GlyRs (Castillo et al., 2009). We recently showed that in ρ1 $GABA_C$Rs, retaining six C-terminal residues of the putative α-helix, including the di-leucine motif, partially restored functional receptors that were

abolished by complete deletion of the α-helix (Wong et al., 2014). Thus, whilst the N-terminal α-helix is consistently shown to contribute to the appearance of functional receptors at the cell surface for a variety of pLGICs, the degree of this contribution and the role of particular residues or segments differ between pLGICs.

N-terminal α-helix deletions had minor effects on $GABA_AR$ functional charateristics

Although deletions of the subunit N-terminal regions markedly reduced the number of functional receptors at the cell surface, they had relatively minor effects on the functional characteristics of the remaining receptors, including GABA EC_{50}, Hill coefficient and desensitization rate. It should be noted that in the experimental system used here, the rate of solution exchange will limit detection of changes in faster components of desensitization. None of the deletions investigated here had any significant effect on the Hill coefficient for GABA activation. Furthermore, no single subunit deletion of the N-terminal extension affected the GABA EC_{50}. Larger single-subunit deletions of the N-terminal α-helix did reduce the sensitivity to GABA (2.5 to 8-fold higher EC_{50}), but only when in the β subunit. Conversely N-terminal deletions in all subunits slightly decreased the GABA EC_{50}, although this was on a background of very small currents. Likewise, it was only in the β subunit that deletions in the α-helix showed small but significant effects on the rate of desensitization. The specific role of the β subunit α-helix in these functional characteristics may be linked to the β subunit contributing the principal face of the GABA-binding site. As the N-terminal helix is not close to the GABA-binding site, it is likely to contribute to conformational changes of GABA-activated gating, rather than directly to GABA binding. Indeed, recent structural comparison of GluCl in various open and closed conformations shows distinct movements at the N-terminal α-helix (Althoff et al., 2014).

Conclusions

In conclusion, our results demonstrate a significant contribution of the N-terminal extension, specifically in the α subunit, to the appearance of functional receptors at the cell surface. The N-terminal α-helices in all subunits also contribute to receptor maturation, with those in the β and γ subunits being important for γ subunit incorporation into $GABA_ARs$. Our data do not define which steps of subunit folding, receptor assembly or trafficking to the cell surface are

particularly affected. As we saw no effect of any deletion on the total expression of the other two subunits, it appears that intracellular subunits that are folded but incompletely assembled are relatively stable and not subject to degradation, consistent with previous findings (Castillo et al., 2009; Wong et al., 2014). The importance of this N-terminal region to $GABA_AR$ function in the brain is highlighted by the identification of epilepsy-linked mutations γ2R43Q, just after the N-terminal α-helix, and β3G7R (Gurba et al., 2012), in the N-terminal extension, both in patients with febrile seizures and childhood absence epilepsy. Both mutations alter subunit composition and reduce receptor levels at the plasma membrane (Frugier et al., 2007; Gurba et al., 2012; Kang and Macdonald, 2004; Sancar and Czajkowski, 2004; Tan et al., 2007; Wimmer et al., 2010).

Acknowledgements

We thank the flow cytometry core facility at School of Medical Sciences, RMIT University. Research was approved by RMIT University and supported by the National Health and Medical Research Council (566672 to BAC) and ANZ Trustees. The authors have no conflicts of interest to declare.

References

Althoff T, Hibbs RE, Banerjee S and Gouaux E (2014) X-ray structures of GluCl in apo states reveal a gating mechanism of Cys-loop receptors. *Nature* **512**:333-337.

Angelotti TP, Uhler MD and Macdonald RL (1993) Assembly of GABAA receptor subunits: analysis of transient single-cell expression utilizing a fluorescent substrate/marker gene technique. *J Neurosci* **13**:1418-1428.

Baburin I, Khom S, Timin E, Hohaus A, Sieghart W and Hering S (2008) Estimating the efficiency of benzodiazepines on GABA(A) receptors comprising gamma1 or gamma2 subunits. *Br J Pharmacol* **155**:424-433.

Bar-Lev DD, Degani-Katzav N, Perelman A and Paas Y (2011) Molecular dissection of Cl--selective Cys-loop receptor points to components that are dispensable or essential for channel activity. *J Biol Chem* **286**:43830-43841.

Barnard EA, Skolnick P, Olsen RW, Mohler H, Sieghart W, Biggio G, Braestrup C, Bateson AN and Langer SZ (1998) International Union of Pharmacology. XV. Subtypes of gamma-aminobutyric acidA receptors: classification on the basis of subunit structure and receptor function. *Pharmacol Rev* **50**:291-313.

Baumann SW, Baur R and Sigel E (2001) Subunit arrangement of gamma-aminobutyric acid type A receptors. *J Biol Chem* **276**:36275-36280.

Bocquet N, Nury H, Baaden M, Le Poupon C, Changeux J-P, Delarue M and Corringer P-J (2009) X-ray structure of a pentameric ligand-gated ion channel in an apparently open conformation. *Nature* **457**:111-114.

Boileau AJ, Baur R, Sharkey LM, Sigel E and Czajkowski C (2002) The relative amount of cRNA coding for gamma2 subunits affects stimulation by benzodiazepines in GABA(A) receptors expressed in Xenopus oocytes. *Neuropharmacol* **43**:695-700.

Boileau AJ, Li T, Benkwitz C, Czajkowski C and Pearce RA (2003) Effects of gamma2S subunit incorporation on GABAA receptor macroscopic kinetics. *Neuropharmacol* **44**:1003-1012.

Bollan K, Robertson LA, Tang H and Connolly CN (2003) Multiple assembly signals in gamma-aminobutyric acid (type A) receptor subunits combine to drive receptor construction and composition. *Biochem Soc Trans* **31**:875-879.

Brejc K, van Dijk WJ, Klaassen RV, Schuurmans M, van Der Oost J, Smit AB and Sixma TK (2001) Crystal structure of an ACh-binding protein reveals the ligand-binding domain of nicotinic receptors. *Nature* **411**:269-276.

Castillo M, Mulet J, Aldea M, Gerber S, Sala S, Sala F and Criado M (2009) Role of the N-terminal alpha-helix in biogenesis of alpha7 nicotinic receptors. *J Neurochem* **108**:1399-1409.

Chen Q, Yim P, Yuan N, Johnson J, Cook J, Smith S, Ionescu Zanetti C, Wang Z-J, Arnold L and Emala C (2012) Comparison of cell expression formats for the characterization of GABA(A) channels using a microfluidic patch clamp system. *Assay Drug Dev Technol* **10**:325-335.

Cole C, Barber J and Barton G (2008) The Jpred 3 secondary structure prediction server. *Nucleic Acids Res* **36**:W197-W201.

Cromer BA, Morton CJ and Parker MW (2002) Anxiety over GABA(A) receptor structure relieved by AChBP. *Trends Biochem Sci* **27**:280-287.

Draguhn A, Verdorn TA, Ewert M, Seeburg PH and Sakmann B (1990) Functional and molecular distinction between recombinant rat GABAA receptor subtypes by Zn2+. *Neuron* **5**:781-788.

Ernst M, Bruckner S, Boresch S and Sieghart W (2005) Comparative models of GABAA receptor extracellular and transmembrane domains: important insights in pharmacology and function. *Mol Pharmacol* **68**:1291-1300.

Eshaq RS, Stahl LD, Stone R, 2nd, Smith SS, Robinson LC and Leidenheimer NJ (2010) GABA acts as a ligand chaperone in the early secretory pathway to promote cell surface expression of GABAA receptors. *Brain Res* **1346**:1-13.

Frugier G, Coussen Fo, Giraud M-F, Odessa M-Fo, Emerit M, Boue-Grabot E and Garret M (2007) A gamma 2(R43Q) mutation, linked to epilepsy in humans, alters GABAA receptor assembly and modifies subunit composition on the cell surface. *J Biol Chem* **282**:3819-3828.

Golden AP, Li N, Chen Q, Lee T, Nevill T, Cao X, Johnson J, Erdemli G, Ionescu-Zanetti C, Urban L and Holmqvist M (2011) IonFlux: a microfluidic patch clamp system evaluated with human Ether-a-go-go related gene channel physiology and pharmacology. *Assay Drug Dev Technol* **9**:608-619.

Gunther U, Benson J, Benke D, Fritschy JM, Reyes G, Knoflach F, Crestani F, Aguzzi A, Arigoni M and Lang Y (1995) Benzodiazepine-insensitive mice generated by targeted disruption of the gamma 2 subunit gene of gamma-aminobutyric acid type A receptors. *Proc Natl Acad Sci USA* **92**:7749-7753.

Gurba K, Hernandez C, Hu N and Macdonald R (2012) GABRB3 mutation, G32R, associated with childhood absence epilepsy alters α1β3γ2L γ-aminobutyric acid type A (GABAA) receptor expression and channel gating. *J Biol Chem* **287**:12083-12097.

Hassaine G, Deluz C, Grasso L, Wyss R, Tol MB, Hovius R, Graff A, Stahlberg H, Tomizaki T, Desmyter A, Moreau C, Li XD, Poitevin F, Vogel H and Nury H (2014) X-ray structure of the mouse serotonin 5-HT3 receptor. *Nature* **512**:276-281.

Hibbs RE and Gouaux E (2011) Principles of activation and permeation in an anion-selective Cys-loop receptor. *Nature* **474**:54-60.

Hilf RJC and Dutzler R (2008) X-ray structure of a prokaryotic pentameric ligand-gated ion channel. *Nature* **452**:375-379.

Hilf RJC and Dutzler R (2009) Structure of a potentially open state of a proton-activated pentameric ligand-gated ion channel. *Nature* **457**:115-118.

Horenstein J and Akabas MH (1998) Location of a high affinity Zn2+ binding site in the channel of alpha1beta1 gamma-aminobutyric acidA receptors. *Mol Pharmacol* **53**:870-877.

Hosie A, Dunne E, Harvey R and Smart T (2003) Zinc-mediated inhibition of GABA(A) receptors: discrete binding sites underlie subtype specificity. *Nat Neurosci* **6**:362-369.

Jordan M and Wurm F (2004) Transfection of adherent and suspended cells by calcium phosphate. *Methods* **33**:136-143.

Kang J-Q and Macdonald R (2004) The GABAA receptor gamma2 subunit R43Q mutation linked to childhood absence epilepsy and febrile seizures causes retention of alpha1beta2gamma2S receptors in the endoplasmic reticulum. *J Neurosci* **24**:8672-8677.

Klausberger T, Ehya N, Fuchs K, Fuchs T, Ebert V, Sarto I and Sieghart W (2001) Detection and binding properties of GABA(A) receptor assembly intermediates. *J Biol Chem* **276**:16024-16032.

Korpi ER, Grunder G and Luddens H (2002) Drug interactions at GABA(A) receptors. *Prog Neurobiol* **67**:113-159.

Krishek BJ, Moss SJ and Smart TG (1996) Homomeric beta 1 gamma-aminobutyric acid A receptor-ion channels: evaluation of pharmacological and physiological properties. *Mol Pharmacol* **49**:494-504.

Macdonald RL and Olsen RW (1994) GABAA receptor channels. *Annu Rev Neurosci* **17**:569-602.

Miller PS and Aricescu AR (2014) Crystal structure of a human GABAA receptor. *Nature* **512**:270-275.

Miyazawa A, Fujiyoshi Y and Unwin N (2003) Structure and gating mechanism of the acetylcholine receptor pore. *Nature* **423**:949-955.

Olsen R and Sieghart W (2009) GABA A receptors: subtypes provide diversity of function and pharmacology. *Neuropharmacology* **56**:141-148.

Pritchett DB, Sontheimer H, Shivers BD, Ymer S, Kettenmann H, Schofield PR and Seeburg PH (1989) Importance of a novel GABAA receptor subunit for benzodiazepine pharmacology. *Nature* **338**:582-585.

Rabow LE, Russek SJ and Farb DH (1995) From ion currents to genomic analysis: recent advances in GABAA receptor research. *Synapse* **21**:189-274.

Reynolds D, Rosahl T, Cirone J, O'Meara G, Haythornthwaite A, Newman R, Myers J, Sur C, Howell O, Rutter AR, Atack J, Macaulay A, Hadingham K, Hutson P, Belelli D, Lambert J, Dawson G, McKernan R, Whiting P and Wafford K (2003) Sedation and anesthesia mediated by distinct GABA(A) receptor isoforms. *J Neurosci* **23**:8608-8617.

Sancar F and Czajkowski C (2004) A GABAA receptor mutation linked to human epilepsy (gamma2R43Q) impairs cell surface expression of alphabetagamma receptors. *J Biol Chem* **279**:47034-47039.

Sarto Jackson I and Sieghart W (2008) Assembly of GABA(A) receptors (Review). *Mol Membr Biol* **25**:302-310.

Saxena NC and Macdonald RL (1994) Assembly of GABAA receptor subunits: role of the delta subunit. *J Neurosci* **14**:7077-7086.

Sieghart W (1995) Structure and pharmacology of gamma-aminobutyric acidA receptor subtypes. *Pharmacol Rev* **47**:181-234.

Sigel E, Baur R, Trube G, Mohler H and Malherbe P (1990) The effect of subunit composition of rat brain GABAA receptors on channel function. *Neuron* **5**:703-711.

Sigel E and Buhr A (1997) The benzodiazepine binding site of GABAA receptors. *Trends Pharmacol Sci* **18**:425-429.

Spencer CI, Li N, Chen Q, Johnson J, Nevill T, Kammonen J and Ionescu Zanetti C (2012) Ion channel pharmacology under flow: automation via well-plate microfluidics. *Assay Drug Dev Technol* **10**:313-324.

Tan H, Reid C, Single F, Davies P, Chiu C, Murphy S, Clarke A, Dibbens L, Krestel H, Mulley J, Jones M, Seeburg P, Sakmann B, Berkovic S, Sprengel R and Petrou S (2007) Reduced cortical inhibition in a mouse model of familial childhood absence epilepsy. *Proc Natl Acad Sci USA* **104**:17536-17541.

Tasneem A, Iyer LM, Jakobsson E and Aravind L (2005) Identification of the prokaryotic ligand-gated ion channels and their implications for the mechanisms and origins of animal Cys-loop ion channels. *Genome Biol* **6**:R4.

Thompson AJ, Lester HA and Lummis SCR (2010) The structural basis of function in Cys-loop receptors. *Q Rev Biophys* **43**:449-499.

Tretter V, Ehya N, Fuchs K and Sieghart W (1997) Stoichiometry and assembly of a recombinant GABAA receptor subtype. *J Neurosci* **17**:2728-2737.

Unwin N (2005) Refined structure of the nicotinic acetylcholine receptor at 4A resolution. *J Mol Biol* **346**:967-989.

Verdoorn TA, Draguhn A, Ymer S, Seeburg PH and Sakmann B (1990) Functional properties of recombinant rat GABAA receptors depend upon subunit composition. *Neuron* **4**:919-928.

Wimmer VC, Reid CA, So EY, Berkovic SF and Petrou S (2010) Axon initial segment dysfunction in epilepsy. *J Physiol* **588**:1829-1840.

Wong LW, Tae HS and Cromer BA (2014) Role of the rho1 GABA Receptor N-Terminus in Assembly, Trafficking and Function. *ACS Chem Neurosci* **5**:1266-1277.

Wooltorton JR, McDonald BJ, Moss SJ and Smart TG (1997a) Identification of a Zn2+ binding site on the murine GABAA receptor complex: dependence on the second transmembrane domain of beta subunits. *J Physiol (Lond)* **505 (Pt 3)**:633-640.

Wooltorton JR, Moss SJ and Smart TG (1997b) Pharmacological and physiological characterization of murine homomeric beta3 GABA(A) receptors. *Eur J Neurosci* **9**:2225-2235.

Table legends

Table 1: **GABA dose-response parameters and pharmacology of WT and mutant $GABA_ARs$**. Parameters are listed for fits to the Hill equation, $EC_{50,}$ Hill coefficient (n_H), and maximum peak current, normalised to WT α1β2γ2 transfected and measured at the same time within each experiment, from n independent measurements. The degree of CDP potentiation (%) and Zn^{2+} inhibition (%) are from a separate set of n independent measurements. All are shown as mean ± SEM, with asterisks indicating significant differences; ***** $p<0.05$, ****** $p<0.01$, ******* $p<0.001$ and ******** $p<0.0001$ compared to α1β2γ2 WT. "ND" indicates not determined.

Figure legends

Figure 1: N-terminus of $GABA_AR$ subunits; structure predictions and deletion mutants. (**A**) Homology models of the $GABA_AR$ α1β2γ2 (left) and α1β2 (right) stoichiometry, shown in ribbon representation, built on GluCl template (3RIF) and viewed along the symmetry axis from the extracellular side. The α1, β2 and γ2 subunits are shown in red, blue and green, respectively, with (+) and (-) faces of each subunit labelled. N-terminal extensions are shown as random coil in thicker tubes of the same colour as the main subunit, with that of γ2 subunit labelled. Putative N-terminal α-helices are internally highlighted in yellow for all subunits. (**B**) ClustalW alignment of pLGIC N-terminal amino acid sequences (excluding signal peptides) manually adjusted for structural alignment to align a partially conserved di-leucine motif (red text). Highly conserved residues are shown in bold. Protein data bank codes are given for sequences with known structures. Regions highlighted are: start of β sandwich domain (green), N-terminal α-helices from crystal structures (cyan) and Jpred3 α-helix predictions (yellow). (**C**) Amino acid sequences of the N-terminal region of WT and deletion mutants of α1, β2 and γ2 subunits using a consistent colour definition of the putative N-terminal α-helix as in (B). Each deletion is named at left, with deleted residues in brackets.

ΔEx represents deletion of the N-terminal extension. ΔExαH represents deletion of the N-terminal extension and α-helix, while maintaining the di-leucine motif (red text). ΔExαH+3 represents deletion of the N-terminal extension and α-helix, including the di-leucine motif.

Figure 2: **Effect of N-terminal extension deletions on GABA sensitivity.** (**A**) Representative population whole-cell currents from HEK-293T cells expressing α1β2γ2, α1(ΔEx)β2γ2, α1β2(ΔEx)γ2 and α1β2γ2(ΔEx) $GABA_A$Rs. The indicated concentrations of GABA (μM) were applied for 3 s to HEK cells voltage-clamped at -80 mV. (**B**) Normalised GABA dose-response curves for cells expressing α1β2γ2 (dashed curve fit) and α1β2 (dotted curve fit), α1(ΔEx)β2γ2, α1β2(ΔEx)γ2 and α1β2γ2(ΔEx) $GABA_A$Rs. Error bars indicate ± SEM. Curves are Hill equation fits of each data set.

Figure 3: **Effect of N-terminal extension deletions on cell-surface and total α and γ subunits detected using flow cytometry.** (**A**) Top: Immuno-fluorescence intensity histograms of cell surface or total anti-α detection for intact or permeabilised HEK-293T cells, respectively. Cells were either untransfected (black) or transfected with α1β2γ2 (red), α1β2ΔExγ2 (green) or α1β2γ2ΔEx (blue) subunits. Below: average population mean fluorescence relative to α1β2γ2 (as %) from 4-5 separate experiments. Error bars indicate ± SEM. (**B**) Top: Immuno-fluorescence intensity histograms of cell surface and total anti-γ2 detection, as for (A), with untransfected (black) or transfected with α1β2γ2 (red), α1(ΔEx)β2γ2 (green) or α1β2(ΔEx)γ2 (blue) subunits. Below: average population mean fluorescence relative to α1β2γ2 (as %) from 4-5 separate experiments. Error bars indicate ± SEM. **** $p<0.0001$ compared to α1β2γ2.

Figure 4: **Effect of N-terminal extension deletions on γ2 incorporation into functional $GABA_A$Rs.** (**A**) Representative population whole-cell currents (black) in response to 1 mM GABA (black line) from HEK-293T cells expressing α1β2γ2, α1(ΔEx)β2γ2, α1β2(ΔEx)γ2, α1β2γ2(ΔEx) or α1β2 subunits (left to right). Overlayed are whole-cell currents (grey) in response to 1 mM GABA in the presence of and pre-incubated with 30 μM Zn^{2+} (grey line). (**B**) Representative population whole-cell currents from HEK-293T cells expressing α1β2γ2, α1(ΔEx)β2γ2, α1β2(ΔEx)γ2, α1β2γ2(ΔEx) or α1β2 $GABA_A$Rs (from left to right) elicited by 6 μM GABA (black line) or subsequent application of 1 μM CDP together with 6 μM GABA (grey dashed line).

Figure 5: **Effect of deletions to the putative α-helix on GABA sensitivity.** Normalised GABA dose-response curves for cells expressing α1β2γ2 (dashed curve fit) and α1β2 (dotted curve fit), reproduced in all panels, together with: (**A**) α1(ΔExαH)β2γ2, α1β2(ΔExαH)γ2 and α1β2γ2(ΔExαH) (**B**) α1β2(ΔExαH+3)γ2 and **(C)** allΔEx α1β2γ2 and allΔExαH α1β2γ2 $GABA_A$Rs. Error bars indicate ± SEM. Curves are fits to the Hill equation of each data set.

Figure 6: **Effect of putative α-helix deletions on cell surface receptors and γ2 incorporation.** Above**:** immunofluorescent detection of (**A**) α1 subunits from α1β2(ΔExαH)γ2- and α1β2γ2(ΔExαH)-expressing cells, and **(B)** γ2 subunits from α1(ΔExαH)β2γ2- and α1β2(ΔExαH)γ2-expressing cells. Data shown are average population mean cell surface or total immunofluorescence from intact or permeabilised HEK-293T cells, respectively, expressed as a % of α1β2γ2 WT, from 3-4 separate experiments in each case. Error bars indicate ± SEM. ** $p<0.01$, *** $p<0.001$ and **** $p<0.0001$ compared to α1β2γ2.

Representative fluorescence histograms for A and B are shown in Supplementary Figure 2. Below: representative population whole-cell currents from HEK-293T cells expressing α1β2γ2, α1(ΔExαH)β2γ2, α1β2(ΔExαH)γ2, α1β2γ2(ΔExαH) and α1β2 $GABA_A$Rs (left to right). (**C**) Sensitivity to Zn^{2+} inhibition, with response to 1 mM GABA (black line) or to 1 mM GABA together with, and preincubated in, 30 μM Zn^{2+} (grey line). (**D**) Sensitivity to CDP potentiation, with response to 6 μM GABA (black line) or to 1 μM CDP together with 6 μM GABA (grey dashed line).

Construct	GABA EC_{50} (μM)	Hill Coefficient (n_H)	Maximum current, I_{MAX} (% of α1β2γ2)	n	CDP potentiation (%)	Zn^{2+} inihibition (%)	n
α1β2γ2	11.0 ± 1.2	1.1 ± 0.1	100	5	54 ± 5	18 ± 2	8
α1β2	0.5 ± 0.2****	0.9 ± 0.2	86 ± 6	5	1 ± 1****	79 ± 2****	4
α1(ΔEx)β2γ2	11.1 ± 0.5	1.2 ± 0.1	16 ± 5****	4	46 ± 10	15 ± 4	3
α1β2(ΔEx)γ2	8.0 ± 0.5	1.3 ± 0.1	81 ± 8	4	39 ± 7	13 ± 4	5
α1β2γ2(ΔEx)	8.0 ± 1.0	1.2 ± 0.1	89 ± 14	4	45 ± 7	19 ± 4	6
α1(ΔExαH)β2γ2	5 ± 2*	1.0 ± 0.3	10 ± 3****	4	48 ± 6	21 ± 5	4
α1β2(ΔExαH)γ2	28 ± 4*	1.0 ± 0.1	40 ± 3****	4	15 ± 4****	43 ± 3****	5
α1β2γ2(ΔExαH)	7.2 ± 1.8	1.0 ± 0.2	70 ± 6**	5	5 ± 2****	61 ± 5****	5
α1(ΔExαH+3)β2γ2	-	-	9 ± 1****	4	ND	ND	
α1β2(ΔExαH+3)γ2	91 ± 19****	1.0 ± 0.1	40 ± 2****	4	ND	ND	
allΔEx	3.9 ± 1.1**	1.1 ± 0.2	12 ± 2****	6	ND	ND	
allΔExαH	1.2 ± 0.6****	1.7 ± 0.6	10 ± 2****	3	ND	ND	

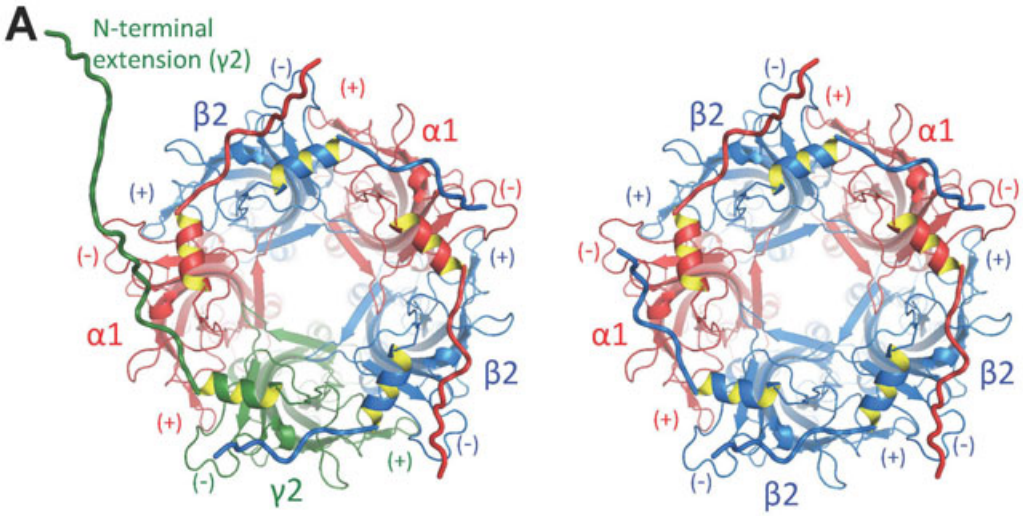

B

```
C.eleg.  GluCl (3RIF)  QQARTKSQDIFEDDNDNGTTTLESLARLTSPIHIPIEQPQTSDSKILAHLFTS GYDFRVRP
L.stagn. AChBP (1I9B)                                      LDRADILYNIRQT  SRPDVIP
T.marm. nAChR α1(4AQ5)                                    SEHETRLVANLLEN  YNKVIRP
Mouse nAChR  α1(2QC1)                                     SEHETRLEAKLFE  DYSSVVRP
Human GABAAR β3(4COF)                                QSVNDPGNMSFVKETVDKLLK  GYDIRLRP
Human nAchR  α7                                           GEFQRRLYKELVK  NYNPLERP
Human GABAAR α1                                  QPSLQDELKDNTTVFTRILDRLLD  GYDNRLRP
Human GABAAR β2                                       QSVNDPSNMSLVKETVDRLLK  GYDIRLRP
Human GABAAR γ2                            QKSDDDYEDYASNKTWVLTPKVPEGDVTVILNNLLE  GYDNKLRP
Human GABACR ρ1 TESRMHWPGREVHEMSKKGRPQRQRREVHEDAHKQVSPILRRSPDITKSPLTKSEQLLRIDDHDFSMRP
```

predicted N-terminal extension

C

predicted N-terminal extension

```
GABAAR α1                                  QPSLQDELKDNTTVFTRILDRLLDGYDNRLRP
α1ΔEx     (Del 2-12)                           QTVFTRILDRLLDGYDNRLRP
α1ΔExαH   (Del 2-21)                                 QLLDGYDNRLRP
α1ΔExαH+3(Del 2-24)                                    QGYDNRLRP

GABAAR β2                                QSVNDPSNMSLVKETVDRLLKGYDIRLRP
β2ΔEx     (Del 2-9)                          QSLVKETVDRLLKGYDIRLRP
β2ΔExαH   (Del 2-18)                                 QLLKGYDIRLRP
β2ΔExαH+3(Del 2-21)                                    QGYDIRLRP

GABAAR γ2                      QKSDDDYEDYASNKTWVLTPKVPEGDVTVILNNLLEGYDNKLRP
γ2ΔEx     (Del 2-24)                           QGDVTVILNNLLEGYDNKLRP
γ2ΔExαH   (Del 2-33)                                 QLLEGYDNKLRP
```

Fig 2